Feeder-Free Derivation of Induced Pluripotent Stem Cells From Human Immature Dental Pulp Stem Cells

Patrícia C. B. Beltrão-Braga,*†‡ Graciela C. Pignatari,†‡ Paulo C. Maiorka,†
Nélio A. J. Oliveira,§ Nelson F. Lizier,‡¶ Cristiane V. Wenceslau,†‡
Maria A. Miglino,†‡ Alysson R. Muotri,§ and Irina Kerkis‡¶

*School of Arts, Science and Humanities, Department of Obstetrics, University of São Paulo, São Paulo, Brazil
†Faculty of Veterinary Medicine, Department of Surgery and Department of Pathology, University of São Paulo, São Paulo, Brazil
‡National Institute of Science and Technology in Stem Cell and Cell Therapy (INCTC), Ribeirão Preto, Brazil
§Department of Pediatrics/Rady Children's Hospital San Diego, Department of Cellular & Molecular Medicine,
Stem Cell Program, School of Medicine, University of California San Diego, La Jolla, CA, USA
¶Butantan Institute, Laboratory of Genetics, São Paulo, Brazil

Induced pluripotent stem cells (iPSCs) can be created by forcing expression of certain genes in fibroblasts or other somatic cell types, reversing them to a pluripotent state similar to that of embryonic stem cells (ESC). Here, we used human immature dental pulp stem cells (hIDPSCs) as an alternative source for creating iPSC. hIDPSCs can be easily isolated from accessible tissue of young and adult patients. hIDPSCs possess a fibroblast-like morphology, retaining characteristics of adult multipotent stem cells. Reprogramming of hIDPSCs was fast, producing primary hIDPSC-iPSC colonies even under feeder-free conditions. hIDPSCs acquired ESC-like morphology, expressed pluripotent markers, possessed stable, normal karyotypes, and demonstrated the ability to differentiated in vitro and in vivo. Our data demonstrate that hIDPSCs-iPSCs offer an advantageous cell system for future cell therapy and basic studies, particularly as a model for pediatric developmental disorders.

Key words: Induced pluripotent stem cells (iPSCs); Pediatric diseases;
Human immature dental pulp stem cells (hIDPSCs); Reprogramming

INTRODUCTION

Induced pluripotent stem cells (iPSCs) can be derived from several adult tissues (1,10,19,30,31,33,35,37). Research involving production of iPSCs is being developed around the world and will likely stimulate the development of several areas of biology and medicine. After reprogramming, somatic cells acquire properties of embryonic stem cells (ESCs) in respect to morphology, proliferation, gene expression, epigenetic profile, and differentiation potential (32). This approach allows for the creation of patient-specific pluripotent stem cells, advantageous for future cell therapy due to immune compatibility. Human iPSCs have been derived from skin fibroblasts, keratinocytes, blood progenitors, and from several types of adult stem cells, such as adipose,

cord blood, neural, and dental pulp (1,10,19,22,30–32, 36,37). Production of iPSCs opens new opportunities for increased understanding of human genetic diseases and embryogenesis, and will likely have a great impact on future drug screening and toxicological tests (21).

However, the reprogramming methodology for derivation of iPSCs is relatively new and needs refining in terms of technique, efficiency, and cell type choice. For example, reprogramming efficiency reported for human fibroblasts is relatively low, while the reprogramming process for keratinocytes generates iPSC colonies 100-fold more efficiently and twofold faster compared to human fibroblasts. Such difference in efficiency is probably because keratinocytes have expression levels of stem cell-related genes more similar to ESCs than fibroblasts (1,12). The timing of reprogramming and the factors re-

quired also seem to vary depending on cellular context (1,2,7,10,15,16,22). Furthermore, adult differentiated cells, such as fibroblasts, can potentially accumulate DNA damage caused by sunlight, increasing the chances of tumor formation (25). Another obstacle is the use of mouse embryonic fibroblasts (MEFs), as feeder cells for hiPSCs. Traditionally, undifferentiated hiPSCs, as well as hESCs, are maintained on MEFs, which may hamper the clinical applications of hESCs (27). In addition, the risk of spreading zoonoses and potential for variability of MEF quality are important issues to consider given the long time scale for reprogramming of human cells.

Human adult stem cells, such as mesenchymal stem cells (MSCs), can be isolated from different tissues of adult organisms and are expected to be less exposed to exogenous environmental factors than differentiated cells. Several attempts have been made to reprogram stem cells from human exfoliated deciduous (SHED) (36) and dental pulp stem cells (DPSCs), as well as from adipose tissues (30). However, it seems that all of these cell types did not present significant difference in efficiency or timing of reprogramming compared to human fibroblasts (36).

We previously isolated and characterized a unique population of cells from dental pulp of "baby teeth" (human exfoliated deciduous teeth) and termed them "human immature dental pulp stem cells" (hIDPSCs), due to several differences observed between these cells and previously described DPSCs and SHED (9,14,24). Interestingly, we found that hIDPSCs shared similar characteristics with both MSC and human ESC (14). Similar to MSCs, hIDPSCs present fibroblast-like morphology and are composed of a homogeneous population in respect to expression of typical MSC markers: 96–98% express SH2 (CD105), SH3 and SH4 (CD73) markers (14). hIDPSCs proliferate rapidly, can easily be expanded in vitro, and are highly clonogenic, exhibiting self-renewing properties for long periods in culture. hIDPSCs also express ESC markers such as Pou transcription factor octamer-4 (Oct4) and stage-specific embryonic antigen 3 and 4 (SSEA-3 and -4). Similar to hESCs, hIDPSCs have capacity for spontaneous differentiation through sphere-like structure formation (resembling ESC embryoid bodies). More recently, we showed that hIDPSCs were able to assimilate and function when introduced into different tissues of human/mouse chimeras (29). However, in contrast to hESCs, teratoma formation has never been observed for hIDPSCs (14). Due to the aforementioned properties, we concluded that hIDPSCs are more mature than hESCs, but less mature than MSCs, making them an intermediate type between both of these cells.

Based on recent evidence that nuclear reprogramming efficiency can depend on cell type (1,2,7,10,15,16,22),

we aimed to reprogram hIDPSCs from two unrelated individuals using four Yamanaka's factors. Here, we report that hIDPSCs can be easily reprogrammed into iPSCs in the absence of MEFs. Reprogrammed hIDPSCs-iPSCs continued to have hallmarks of pluripotent cells and attained efficient neuronal differentiation in vitro.

MATERIALS AND METHODS

Ethics Statement

All animal work was conducted according to relevant national and international guidelines. Protocols were previously approved by the University of California San Diego Institutional Animal Care and Use Committee, the Institutional Review Board and the Embryonic Stem Cell Research Oversight Committee, and Institute of Biomedical Science Ethical Committee from University of São Paulo.

Cell Culture

Human IDPSCs ($2n = 46$, XY) were isolated and previously characterized and cultured as described by Kerkis et al. (14). Dental pulp was extracted from normal exfoliated human deciduous teeth of 7-year-old children (two patients) after informed consent. Tissue was then washed twice with sterile phosphate-buffered saline (PBS; 0.01 M, pH 7.4) supplemented with antibiotics (100 U/ml penicillin and 100 µg/ml streptomycin), and transferred (with minimal dissection) to 35-mm petri dishes (Corning, New York, NY, USA) with Dulbecco's modified Eagle's medium (DMEM)/Ham's F12 (1:1, Invitrogen, Carlsbad, CA, USA) supplemented with 15% fetal bovine serum (FBS, HyClone, Logan, UT, USA), 100 U/ml penicillin, 100 µg/ml streptomycin, 2 mM L-glutamine, and 2 mM nonessential amino acids. Tissue explant of dental pulp was used to isolate hIDPSCs. hIDPSC culture was maintained under these conditions for 2 weeks, after which cells were washed twice in PBS, dissociated in a 0.25% trypsin solution (Invitrogen), and seeded at 10^4 cells per 25-cm^2 flask. Subsequent cultures were maintained semiconfluent to prevent differentiation. Cells were passed every 4–5 days with the medium refreshed daily. All cultures were incubated at 37°C in 5% CO_2 in a high-humidity environment. When freezing, cells were ressuspended in medium containing 20% FBS, 70% DMEM, and 10% dimethyl sulfoxide (Sigma, St. Louis, MO, USA) at 5×10^5 cells/ml, and the temperature was slowly and gradually decreased at a rate of 1°C per minute until a final temperature of −70°C was reached. Cells were then transferred to liquid nitrogen.

Flow Cytometry

Flow cytometry was performed using hIDPSCs at passage three. The cells were detached by using a 10-

min treatment at 37°C with PBS 0.02% EDTA (Invitrogen), pelleted (10 min at 1,000 rpm) and washed in 0.1% bovine serum albumin (BSA, Sigma) in 0.1 M PBS (Invitrogen) at 4°C. Next the cells at a concentration of 1.0×10^6 cells/ml were permeabilized with 0.1% Triton X-100 (Sigma) 15 min at room temperature. After that the cells were stained with 1 μg of human antibodies against anti-vimentin phycoerythrin (PE)-conjugated and anti-nestin fluorescein isothiocyanate (FITC)-conjugated (both from Santa Cruz Biotechnology, Santa Cruz, CA, USA). After 45-min incubation in the dark at room temperature, cells were washed three times with PBS and resuspended in 0.25 ml PBS. Isotype-matched controls were done. Cells were then analyzed using a FACS Caliber (Becton-Dickson, Mountain View, CA), Cell Quest software (Becton-Dickson) using 10,000 events.

Retroviruses Preparation

Retroviral vectors containing human cDNA from Yamanaka's group [pMx vectors of Klf4 (Krüppel-like factor), Oct4, c-Myc, and Sox2 (sex determining region Y-box 2)] were obtained from Addgene (www.addgene.org). Retroviruses were produced by triple transfection (one plasmid with cDNA and two auxiliary plasmids for packaging viral particles) of HEK293T cells followed by ultracentrifugation as previously described (34). hIDPSCs were transduced at a titer of approximately 0.5×10^{10} gene transfer U/ml overnight. Based on an enhanced green fluorescent protein (EGFP) reporter virus used in parallel and postinfection immunostainning with antibodies against the reprogramming factors, we estimated that our infection efficiency was 80–95%. After a 2-day recovery period, infected hIDPSCs were plated either on mitotically inactive MEFs as feeder cells, or onto Matrigel-coated (BD, Franklin Lakes, NJ, USA) dishes without feeder cells, in the presence of ESC medium (DMEM/F12 glutamax, 20% KSR, 2 mM nonessential amino acids, 10^{-4} M β-mercaptoetanol) containing 30 ng/ml basic fibroblast growth factor (bFGF-2; Invitrogen). The medium was refreshed every day. For feeder-free hIDPSCs, human ESC medium was conditioned for 24 h in MEFs. The reprogramming was verified by the amount of colonies with hESC morphology at 10 days after reprogramming. Each colony was manually subcloned into wells of 12-well plates seeded with MEFs or coated with Matrigel. Each colony was expanded for further experimental analyses.

Karyotyping

Selected iPSC clones were analyzed at passage 10 and 15. Colcemid (Sigma, 0.02 μg/ml) was added to hIDPSC-iPSC colonies for 1.5 h. Cells were then trypsinized, centrifuged at 1,000 rpm for 5 min, resuspended in 5 ml of 0.075 M KCl, and incubated for 30 min at 37°C. Cells were fixed in ice-cold acetic acid and methanol (1:3 solution). Approximately 30 metaphases from cells were analyzed by G-banding. Karyotypes were analyzed according to the "International System for Human Cytogenetic Nomenclature" using a Zeiss II microscope (Zeiss, Jena, Germany).

Immunocytochemistry

Cells were washed twice in rinse buffer (20 mM Tris-HCl, pH 7.4, 0.15 M NaCl, 0.05% Tween-20), fixed with 4% paraformaldehyde, and permeabilized with 0.1% Triton X-100. After blocking with 5% BSA, the cells were incubated with diluted primary antibodies for 1 h at room temperature. Primary antibodies from the ES Cell Marker Sample Kit were diluted 1:40 and 1:100. After washing three times in rinse buffer, appropriate FITC- or Cy3-labeled secondary antibodies were added for 40 min at 1:100 dilution at room temperature. Microscope slides were mounted in Vectashield mounting medium (Invitrogen) with or without 4′,6-diamidino-2-phenylindole (DAPI; Vector Laboratories, Burlingame, CA, USA). Visualization was achieved using digital images that were acquired with a cooled CCD camera (PCO, VC44) and processed with ISIS software (Meta-System, Belmont, MA, USA). Antibodies against Nanog, Sox2, Klf-4, and c-Myc were obtained from Case Western Reserve University (Cleveland, Ohio, USA) and stage-specific embryonic antigens (SSEA-3 and SSEA-4), and tumor recognition antigens (TRA-1-60 and TRA-1-81), and Oct3/4 were purchased from Chemicon (Temecula, CA., USA). Mouse monoclonal nestin and glial fibrillary acidic protein (GFAP) antibodies were purchased from Santa Cruz Biotechnology (Santa Cruz, CA, USA), β-Tubulin III from Sigma, enolase from DAKO Denmark (Glostrup, Denmark), and the oligodendrocyte marker O4 from Chemicon. Immunostained cells were visualized using a laser scan microscope (LSM 510—Zeiss, Jena, Germany) equipped with an argon ion laser (488 nm for FITC or 536 nm for rhodamine) and long pass filter (505 nm for FITC or 617 nm for rhodamine).

RNA Extraction and RT-PCR

Total RNA was extracted from ~5×10^6 hIDPSCs-iPSCs and control cultures (ESCs) with TRIzol reagent (Invitrogen). cDNAs were synthesized from 1 μg of total RNA reverse transcribed with RevertAid M-MuLV Reverse Transcriptase and oligo(dT) (Fermentas Life Science, Amherst, NY, USA) according to the manufacturer's instructions. RT-PCR for transgene expression was used as described previously in Takahashi et al. (31). The following primers for mesenchymal stem cell marker CD73 gene expression were used for amplification by RT-PCR: hCD73 forward, 5′-′ACA CGG CAT

TAG CTG TTA TT-3′ and hCD73 reverse, 5′-AAG TAT TTG TTC TTT GGG CA-3′ and hGAPDH (glyceraldehyde 3-phosphate dehydrogenase) forward, 5′-ACC ACA GTC CAT GCC ATC AC-3′ and hGAPDH reverse, 5′-TCC ACC ACC CTG TTG CTG TA-3′. PCR reactions were prepared with 50 ng cDNA, 0.2 μM primer, 1 unit Taq DNA Polymerase, 0.2 μM dNTPs, 1.5 mM magnesium chloride, and Taq DNA polymerase buffer (Fermentas Life Science). PCR conditions were: initial denaturation at 94°C for 4 min followed by 30 cycles at 94°C for 1 min, annealing for 1 min at 56°C and 72°C for 1 min, with a final extension at 72°C for 10 min. The hESC line HUES6 was used as control. PCR products were separated by 1.5% agarose gel electrophoresis, stained with ethidium bromide, and visualized by UV transilluminator. DNA markers were used to confirm the size of the resultant fragments.

Quantitative PCR Assay

Quantitative PCR primers and conditions were used as described previously in Takahashi et al. (31).

Teratoma Formation in Nude Mice

Approximately 1×10^6 hIDPSCs-iPSCs or hIDPSCs were suspended in PBS and injected into either the right testicle or intramuscularly into the limb of nude mice anesthetized with isoflurane. The sites of injection were chosen based on reports of ESC teratomas formation assays (5,17). Mice were euthanized using rising CO_2 levels, and tumors were carefully excised and fixed in neutral buffered 10% formalin and processed for routine histological study. Sections (4–5 μm) were cut, using a Leica microtome, and slides were stained with hematoxilin-eosin for histopathological evaluation. Immunostaining was performed using the DAB detection system (Universal LSAB™ Kits and Liquid DAB+, Dako North America Inc., CA, USA). Primary antibodies used were anti-cytokeratin (Clones AE1/AE3, Code M3515, from Dako, 1:50); anti-vimentin (code M0725, from Dako, 1:100); anti-desmin (clone D33, from Dako, 1:50); anti-GFAP (clone Code Z 0334, from Dako, 1:500); anti-synaptophysin (code A0010, from Dako, 1:200); anti-NSE (neuron-specific enolase) (code M0873, from Dako, 1:50). Sections from immunohistochemistry assay were counterstained with Harrys hematoxylin. Periodic Acid of Schiff (PAS) staining was also performed to visualize glycogen cell deposits.

RESULTS

Generation and Characterization of hIDPSCs-iPSCs

Cells isolated from dental pulp of two unrelated patients, after informed consent, produced hIDPSCs-iPSCs. Two cell cultures, denominated hIDPSC7 and

hIDPSC8 (both 46 XY), were isolated and properly characterized. They displayed all properties of hIDPSCs previously described (14). Cells had a fibroblast-like morphology (Fig. 1A) with large nucleus and cytoplasm-poor organelles (Fig. 1B). Expression of Oct3/4 and Nanog proteins was found in both studied hIDPSCs in several single cells or in clusters composed of 3 or 4 cells (Fig. 1C–F). Variation in intensity of fluorescent signal was observed in both hIDPSC cultures (Fig. 1C–F), suggesting different levels of pluripotent protein expression (Fige 1D, D1). Additionally, hIDPSC cultures were tested uniformly immunopositive for expression of vimentin and nestin proteins (Fig. 1G, H) and by FACS analysis (Fig. 1I), indicating their ectomesenchymal origin.

Reprogramming experiments were conducted using retroviruses carrying the four human Yamanaka's factors (Oct4, Sox2, Kfl4, and c-Myc), as previously described (31,32). Cells from hIDPSC7 culture were reprogrammed immediately after isolation at passage 1 (P1), and before cryopreservation, while hIDPSC8 were reprogrammed at P7. Two days after infection, both hIDPSCs were plated onto either a layer of irradiated MEFs or directly onto Matrigel. Colonies derived from each reprogrammed hIDPSCs were designated hIDPSC-iPSC7 and hIDPSC-iPSC8. Cells were mechanically expanded for at least 20 passages. RT-PCR analyses for transgene expression were monitored and both hIDPSC-iPSC7 and hIDPSC-iPSC8 seem to almost completely silence their transgenes (Fig. 2A). A RT-PCR for a MSC marker was performed to confirm genetic reprogramming of hIDPSCs. Both hIDPSC7 and hIDPSC8 were positive for CD73 (SH3), a typical MSC gene, previously demonstrated to be expressed in hIDPSCs (14). After reprogramming, CD73 was downregulated in both iPS clones, at similar levels to hESCs (Fig. 2B). Moreover, quantitative PCR in reprogrammed hIDPSCs revealed a tendency for increasing expression of pluripotent factors Oct4, Sox2, and Nanog, when compared to nonreprogrammed cells (Fig. 2C). Similar to our results, variable levels of pluripotent genes were found in iPSC clones when compared to hESCs, but all clones had levels higher than the original fibroblast cells (4). Taken together, our data strongly suggest that ectopic expression of the four Yamanaka's factors reprogrammed hIDPSCs at the molecular level. Karyotype of cells remained unchanged, suggesting that during reprogramming, numerical and gross structural chromosomal abnormalities did not occur as shown by both routine Giemsa and G-banding techniques (Fig. 2D, E).

Multiple primary colonies of hIDPSC-iPSC7 and hIDPSC-iPSC8 growing in the presence of MEF were observed 5 (Fig. 3A, B) and 11 days after transduction (Fig. 3C, D), both forming large colonies resembling
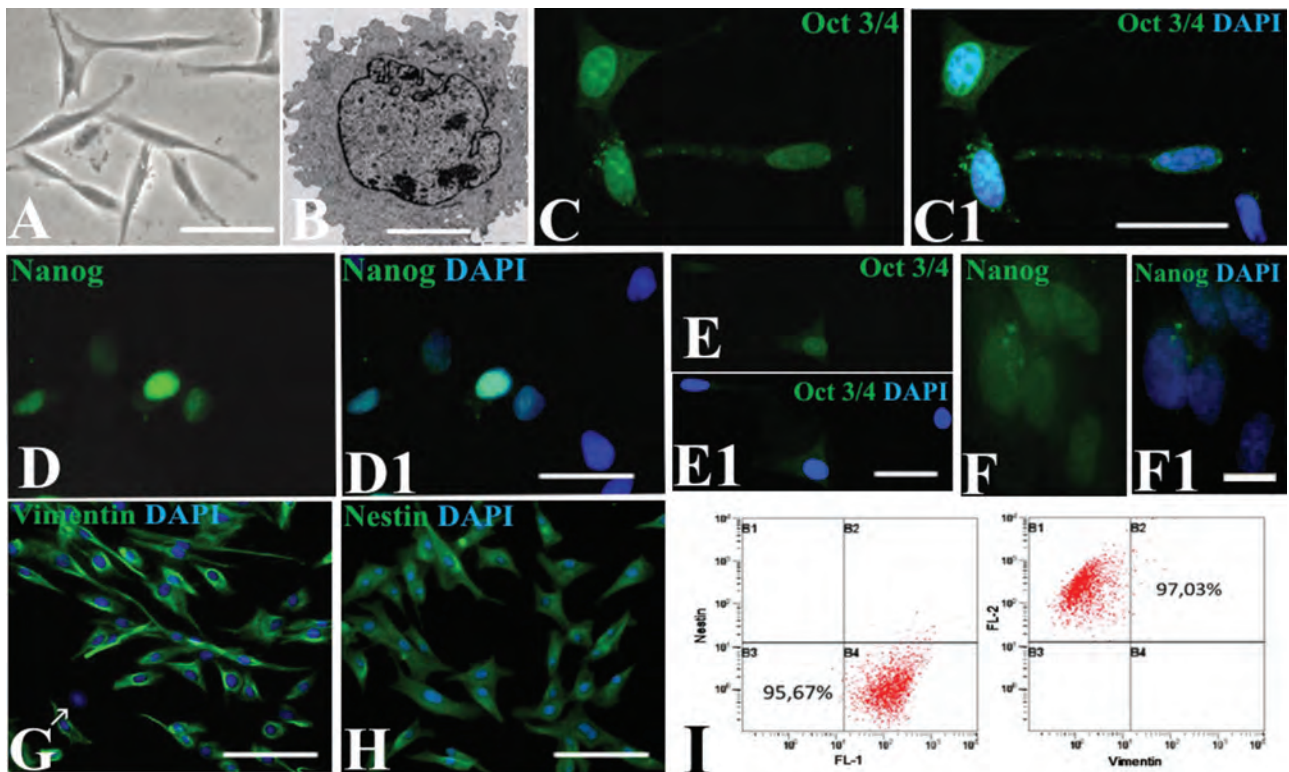
Figure 1. Morphological characteristics and expression profile of pluripotent and adult stem cell key proteins during human immature dental pulp stem cell (hIDPSC) in vitro culturing. (A) Morphology of hIDPSCs (light microscopy). (B) Transmission electron microscopy: hIDPSCs showing large nucleus-to-cytoplasm ratio and prominent nucleoli. Expression of embyronic stem (ES) cell hallmarks in both hIDPSC-DL7 (C, D1) and hIDPSC-DL8 (E, F1) assessed by immunofluorescence (all green): (C, C1) Oct3/4 and (D, D1) Nanog; (E, E1) Oct3/4 and (F, F1) Nanog. Variations or lack of fluorescence signal of both proteins within the cell nuclei. (G, H) Expression of vimentin and nestin proteins in hIDPSC-DL7. Vimentin presents specific cytoskeleton localization and nestin shows stronger fluorescent signal in undifferentiated cells. Nuclei stained with DAPI (blue). (I) Fluorescence activated cell sorting (FACS) analysis of nestin and vimentin expression in hIDPSC-DL7. (C–H) Epifluorescence. Scale bars: 10 µm; (A, C–E1, G, H); 5 µm (B, F1).

hESC colonies. Colonies of hIDPSC-iPSC7 were also observed growing in the absence of MEFs as feeder layer, with 5 and 11 days and 2 months after transduction (Fig. 3E–G). Reprogrammed cells were morphologically indistinguishable from the control hESCs cultured on Matrigel, forming juxtaposed colonies of cells with a large nucleus to cytoplasm ratio and prominent nucleoli (Fig. 3H). The same results without MEFs were observed with the hIDPSC-iPSC8 (Fig. 3I–L). We manually selected only ESC-like undifferentiated colonies, which were propagated under feeder-free conditions on Matrigel-coated dishes until morphologically homogeneous populations of both hIDPSC-iPSC7 and hIDPSC-iPSC8 were achieved.

Before reprogramming, expression of ESC markers was observed only in some hIDPSCs. After 5 days of viral transduction, primary hIDPSC-iPSC colonies or cluster of cells could be seem expressing pluripotent stem cell markers (Fig. 4A–F), as well as observed in large colonies of both hIDPSC-iPSC7 and hIDPSC-iPSC8 lineages after 11 days or 2 months of cell culturing (Fig. 4G–P).

Embryoid Body (EB) Formation and Neuronal In Vitro Differentiation

EBs were created using the hanging drop method, cultured for 3 days, and then allowed to adhere in basal culture medium. After an additional 3 days, EBs showed spontaneous differentiation into skeletal-like muscle and neuronal-like cells (Fig. 5A–C). Previously we demonstrated that hIDPSCs were able to differentiate spontaneously into neurons in the absence of any type of inducers (14). Thus, we decided to test if reprogrammed IDPSCs would behave similarly. Nestin expression was detected in most cells from both hiPSC-IDPSC7 and hiPSC-IDPSC8 colonies (Fig. 5D). EBs were created from these colonies and were transferred to neurobasal culture medium supplemented with B27. After 3 days, EBs
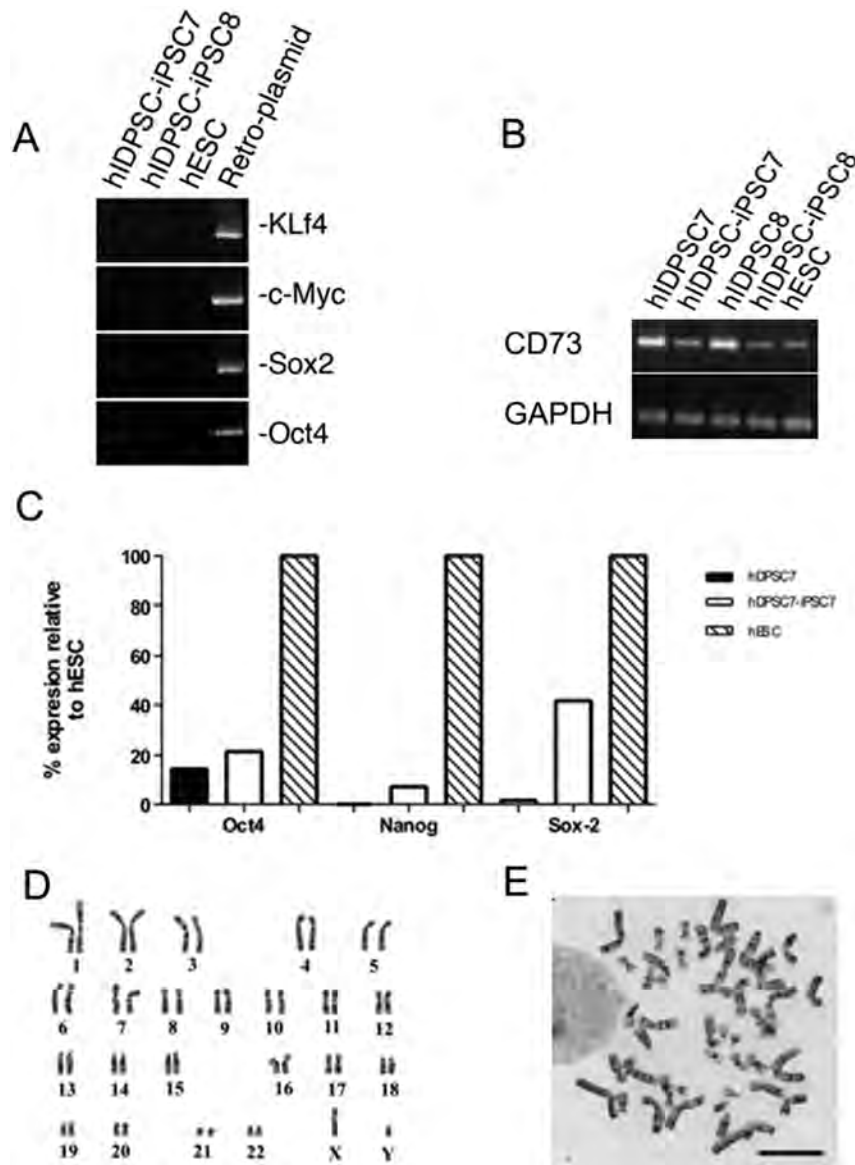
Figure 2. Characterization of hIDPSCs-iPSCs (human immature dental pulp stem cells—induced pluripotent stem cells). Gene expression profile of adult and pluripotent stem cells and karyotype. (A) RT-PCR analyses of hIDPSC-iPSC7 and hIDPSC-iPSC8 transgene expression of Krüppel-like factor 4 (Klf4), c-Myc, sex determining region Y-box 2 (Sox2), and octamer-binding transcription factor 4 (Oct4). Human ES cells and retroviral plasmid were used as controls. (B) RT-PCR analyses of hIDPSCs before and after reprogramming for mesenchymal CD73 (SH3) gene expression. (C) Quantitative PCR of hIDPSC7s before and after reprogramming for endogenous expression of Oct4, Nanog and Sox2 genes. (D) Karyotypes of hIDPSCs-iPSC7s: chromosomes in pairs, ordered by size and position (D) did not reveal any numerical changes in chromosome number; G-banding analysis (E) did not show any chromosomal structural changes. (D, E) Light microscopy (LM). (E) Magnification: 63×; scale bar: 50 μm.

were plated and tested nestin positive when immunolabeled (Fig. 5E). Rosettes formed from these adherent EBs (Fig. 5F, G), and after 1 week a net of terminally differentiated β-tubulin III-positive neuronal-like cells could also be observed (Fig. 5H–J). hIDPSC-iPSC-derived neurons expressed neuron-specific enolase (NSE), which confirmed correct vesicular immunostaining in cytoplasm (Fig. 5K). Glial-like cells were also

observed, which stained positive for glial fibrillary acidic protein (GFAP) (Fig. 5L–O).

Teratoma Formation

We previously reported that hIDPSCs do not have the ability to form teratomas (14). Therefore, both hIDPSC-iPSC7 and hIDPSC-iPSC8, and respectively hIDPSCs (used as controls) were injected into immune-deficient mice to test in vivo pluripotency through teratoma formation. Teratomas were observed between 5 and 7 weeks in mice injected with reprogrammed hIDPSCs-iPSCs, while those inoculated with hIDPSCs, as expected, did not form teratomas. Teratomas contained derivatives from three embryonic germ layers, confirming that both hIDPSC-iPSC7 and hIDPSC-iPSC8 were pluripotent and able to differentiate to complex tissues in vivo. Histological characterization of tumor masses showed diffuse growth and composition of a mosaic of different cell patterns (Figs. 6 and 7). HIDPSC-iPSC teratoma derivates included ectodermal (primitive neural tissues, including neural tube and neural rosettes and retinal epi-

thelium, Fig. 6B, C), mesodermal (muscle-like cells and glomerulus-like structures, Fig. 6D, E), and endodermal tissues (respiratory or gastrointestinal-like epithelium and glandular-like tissue formation, Fig. 6F, G). Teratomas derived from hIDPSC-iPSC7 displayed strong neuronal commitment: development of rosette-, neurosphere-, and neural tube-like structures were observed. Expression of neuron-specific enolase (NSE), which is found in neurons and peripheral neuroendocrine tissue, and synaptophysin (a synaptic vesicle glycoprotein), was detected in neuroendocrine cells and in virtually all neurons in the brain and spinal cord that participate in synaptic transmission (3) (Fig. 7).

DISCUSSION

Somatic cells provide barriers to efficient reprogramming to iPSCs at different stages (1,2,7,10,15,16,22). Mouse hematopoietic cells, depending on stage of differentiation, can be reprogrammed 300 times more efficiently than terminally differentiated B and T cells (7). Our data confirmed previous studies that it seems to be
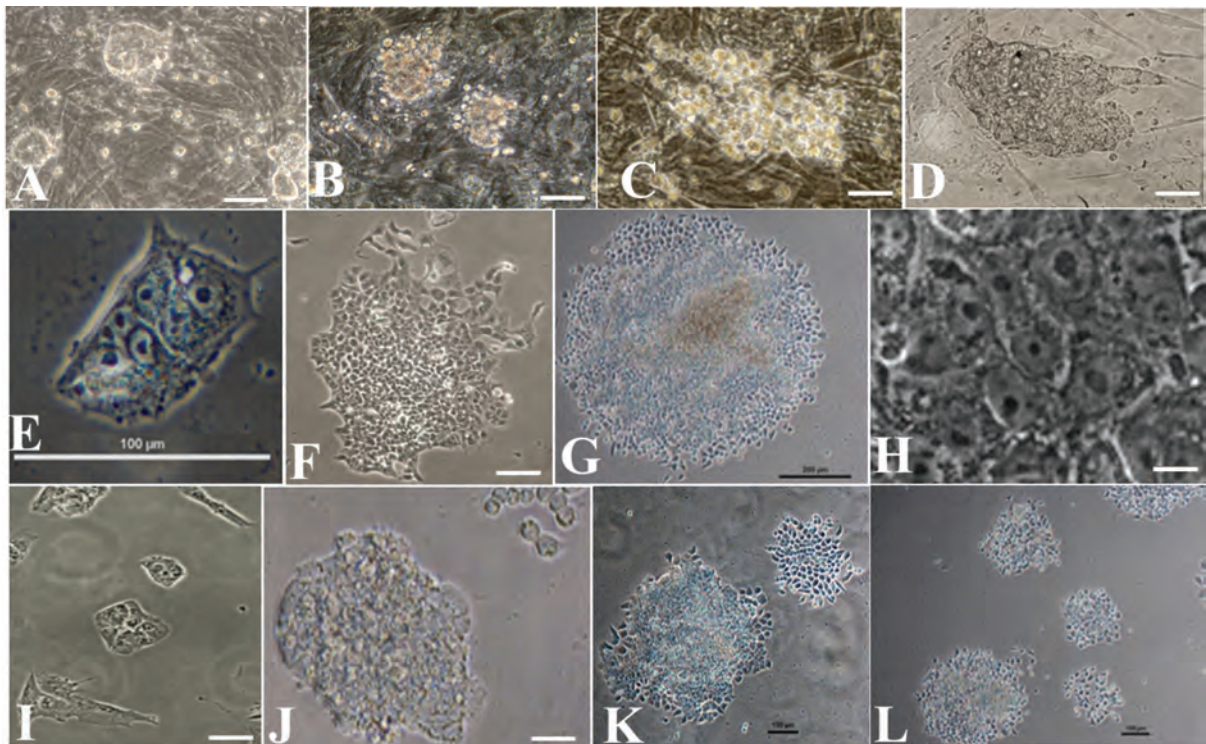
Figure 3. Morphology of hIDPSCs-iPSCs growing on feeder (A–D) and feeder-free colonies (E–L). A, B) Primary colonies of hIDPSC-iPSC7 and hIDPSC-hiPSC8 on mouse embryonic fibroblasts (MEFs) 5 days after transduction, respectively. (C, D) HIDPSC-hiPSC7 and hIDPSC-hiPSC8 colonies growing on MEFs 11 days after transduction, respectively. (E, G) hIDPSC-iPSC7 feeder-free colonies, 5 days, 11 days, and 2 months after transduction, respectively. (H) Morphology of hIDPSC-iPSC7 at higher magnification of (G). (I, J) hIDPSC-iPSC8 feeder-free colonies, 5 days, 11 days, and (K, L) 2 months after transduction. (A–L) Phase Contrast. Scale bars: 50 µm (A–D, F, H–J); 100 µm (E, K, L); 200 µm (G).
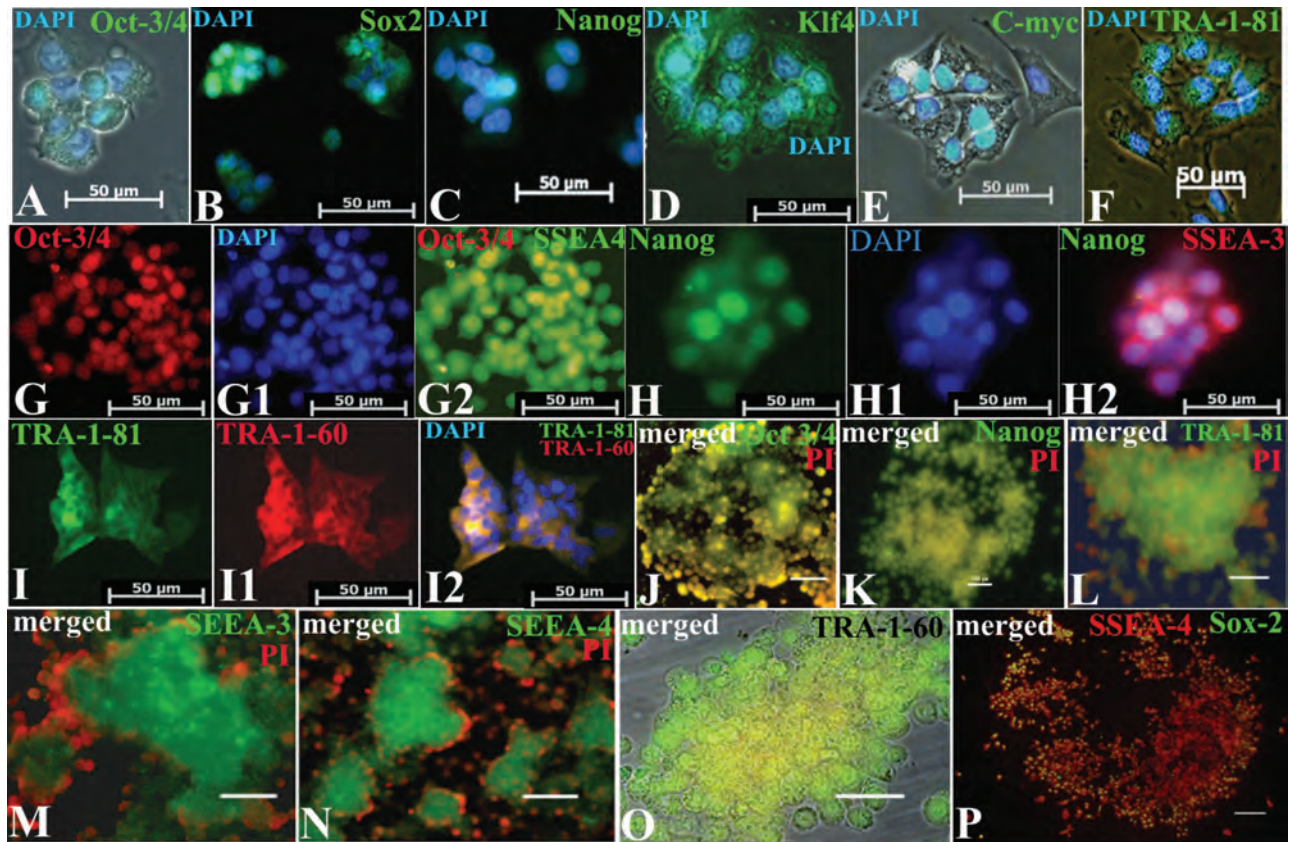
Figure 4. Derivation of iPSCs from hIDPSCs. (A–F) HIDPSC-iPSC7 primary colonies 5 days after transduction expressing pluripotent or transduced genes. Cells immunostained with antibodies against (A) Oct3/4; (B) Sox2; (C) Nanog; (D) Klf4; (E) c-Myc; (F) tumor recognition antigens (TRA)-1-81. (G–I2) Expression of ES cell hallmarks in hIDPSC-iPSC7 colonies 2 months after culturing: (G–G2) expression of Oct3/4 and stage-specific embryonic antigen-4 (SSEA-4) proteins; (H–H2) expression of Nanog and SSEA-3 proteins; (I–I2) expression of TRA-1-81 and TRA-1-60 proteins. Nuclei stained with DAPI (blue). (J–O) Expression of pluripotent hallmarks in hIDPSC-iPSC8 colonies 2 months after culturing: (J) Oct3/4; (K) Nanog; (L) TRA 1-81; (M) SSEA-3; (N) SSEA-4; (O) TRA-1-60 (all green). Nuclei stained with propidium iodide (PI; red). (P) Merged image evidence of coexpression of Sox2 (nuclear localization) and SSEA-4 (cytoplasm localization) within hIDPSC-iPSC8 colony Sox2 (green). (A, D–F, O) Merged image: PC + epifluorescence (Epi); (B–N, P) Epi. Scale bars: 50 µm (A–I2); 100 µm (J–P).

more efficient to reprogram immature rather than terminally differentiated cells (1,22,28). Furthermore, adult human neural stem cells, which express high endogenous levels of Sox2 and c-Myc, can be easily and efficiently reverted to pluripotent state using a single reprogramming factor (22).

We previously reported that stem cells isolated from dental pulp expressed some pluripotent stem cell markers, such as Oct3/4 (14). Other groups have also isolated similar stem cell populations from human dental pulp (11,26). Our data suggest that the genetic profile of hIDPSCs is closer to pluripotent stem cells than to MSCs and terminally differentiated fibroblasts (11,14). Indeed, hIDPSCs were able to functionally contribute to several tissues in human/mouse chimeras when transplanted into mouse blastocysts (29). These findings strongly suggest that hIDPSCs provide a stable foundation for genetic reprogramming similar to that of adult neural stem cells (22).

We have generated hIDPSCs-iPSCs in a short time frame when compared to data reported for other human cells. hIDPSC reprogramming was significantly faster compared to data reported for human fibroblasts, SHED, and DPSCs (36). Furthermore, hIDPSCs-iPSCs are readily obtained and easily expanded in feeder-free conditions, reducing potential for contamination from non-human factors (23,27). All isolated hIDPSC-iPSC colonies proliferated rapidly and were passed every 3–4 days. Normal karyotype was observed in all in vitro cultured hIDPSC-iPSC clones, even after several passages.

Other critical parameter in iPSC generation is the patient's age. Maherali and Hochedlinger (20) and Li and coworkers (18), who compared skin fibroblasts from 2-month-old mice to the same cells from mice aged 2 years

or more, found that older cells produce half as many iPS cells as younger fibroblasts. The fact that hIDPSCs were isolated from dental pulp of young patients may also contribute on the velocity of reprogramming.

The pluripotency of hIDPSCs-iPSCs was verified through teratoma generation in immunodeficient mice. We observed a strong tendency for hIDPSCs-iPSCs to differentiate into the neural lineages, probably reflecting memory retention from its ectomesenchymal nature. This neuronal tendency could be an advantage, espe-
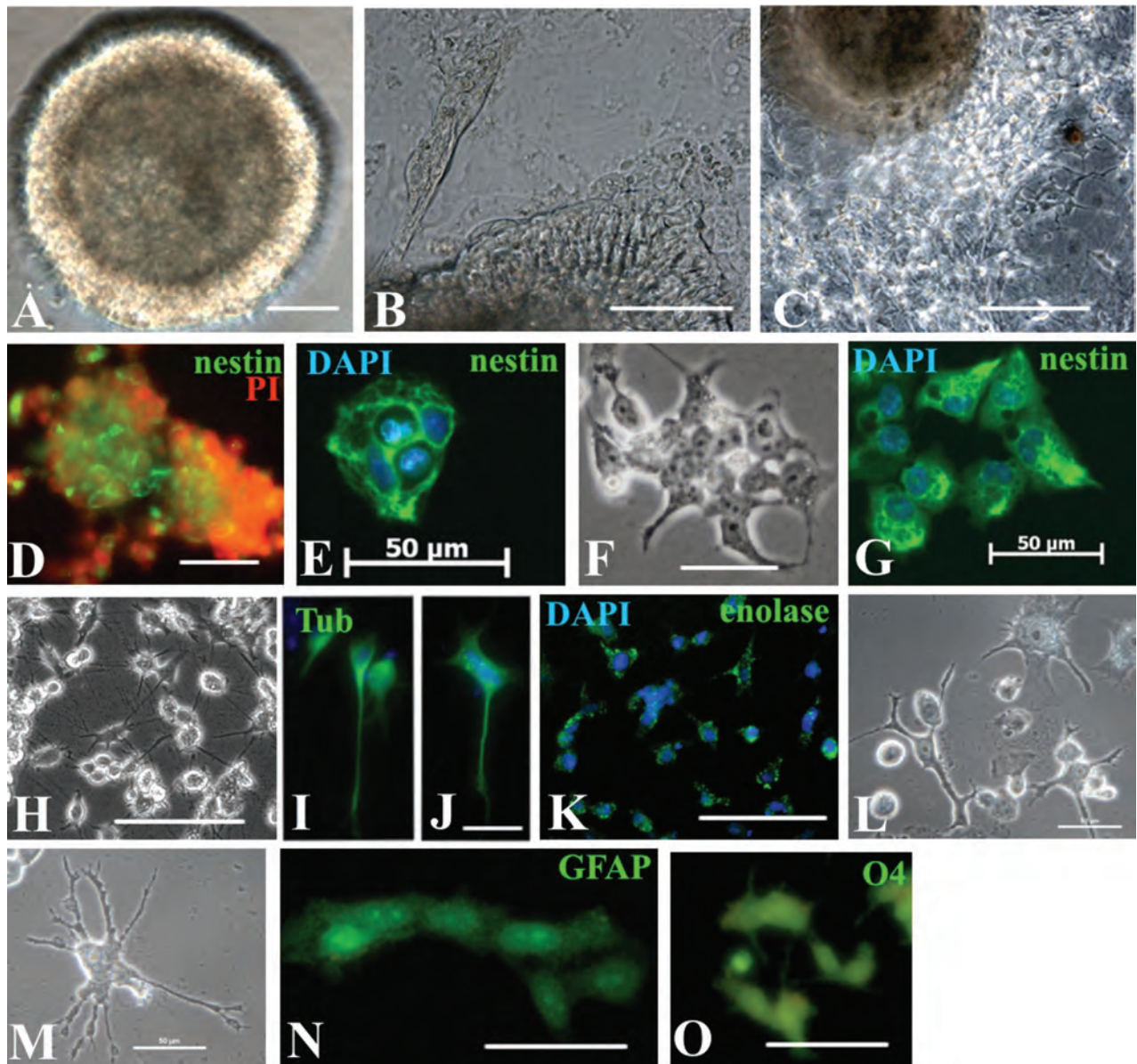
Figure 5. In vitro differentiation of hIDPSCs-iPSCs. (A) Floating embryoid body (EB) formation. (B) EBs adherent on a petri dish showing differentiation to muscle-like cells or differentiation into neuronal-like cells (C). D) Undifferentiated colonies of hIDPSCs-iPSCs, which already present positive immunostaining with anti-nestin antibody. (E) Neuronal differentiation: EBs 3 days after culturing in NB + B27. (F, G) hIDPSC-iPSC neuronal differentiation in progress: formation of rosettes, which express nestin protein. (H) Morphological presentation of advanced stage of neuronal hIDPSC-iPSC differentiation. (I, J) Positive immunostaining with anti-β-tubulin III antibody. (K) Neuron-specific enolase (NSE) expression (green) in hIDPSCs-iPSCs. (L, M) Morphological presentation of glial-like cells derived from hIDPSCs-iPSCs. Expression of anti-GFAP (glial fibrillary acidic protein) (N) and anti-O4 (oligodendrocyte marker 4) (O) antibodies in glial-like cells. Nuclei stained with DAPI (blue). (A–C, F, H, L, M) PC; (D, E, G, I–K, N, O) Epi. Scale bars: 200 μm (A–C); 100 μm (D, H, K); 50 μm (E–G, L, M); 10 μm (I, J); 20 μm (N, O).
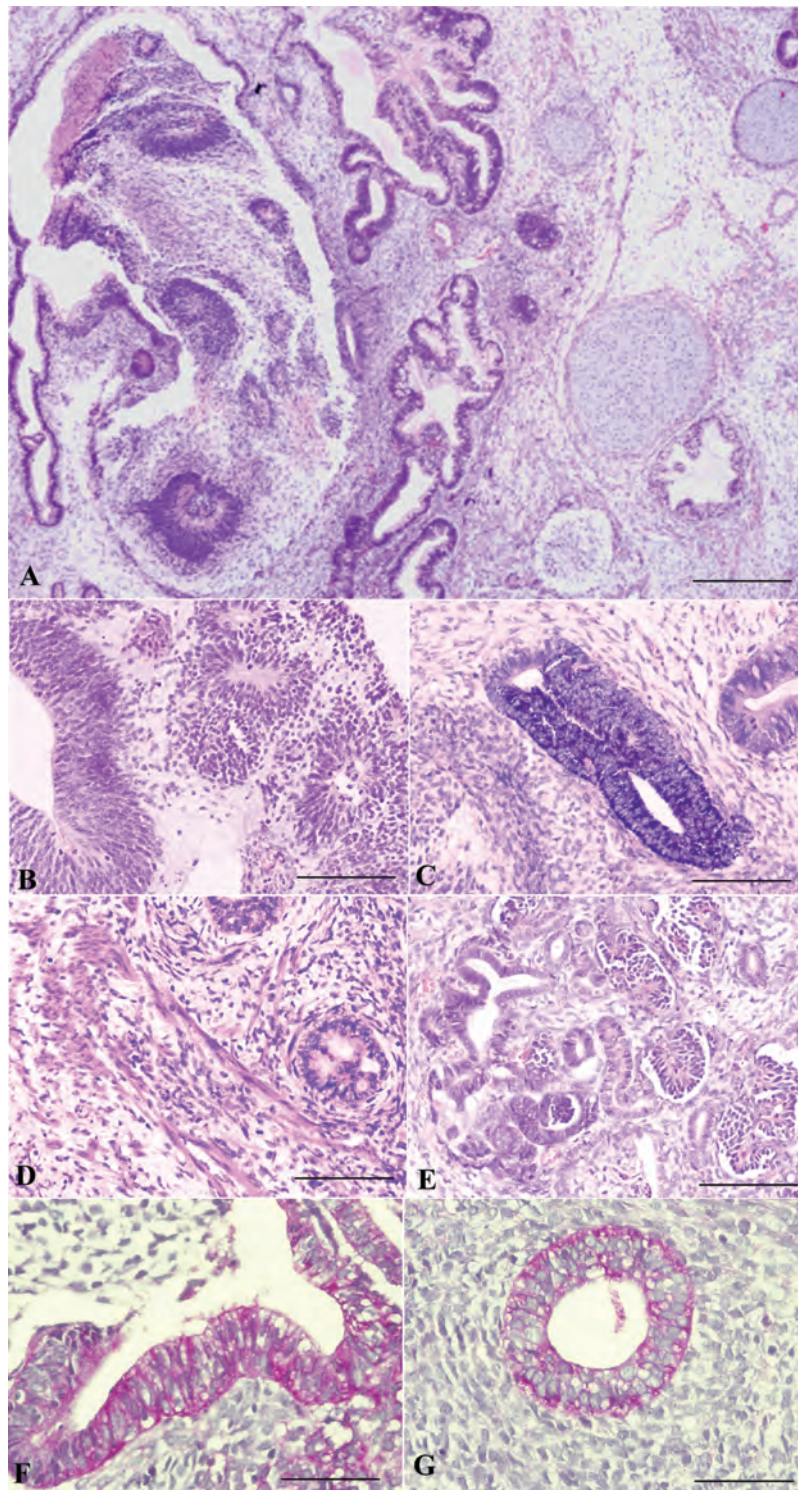
Figure 6. Hematoxylin and eosin stained (H&E) tissue samples of paraformol-fixed teratomas from hIDPSC-iPSC8 7 weeks after intramuscular transplantation into nude mice. (A–G) Morphology of teratoma showing multiples types of differentiated tissues from three embryonic germ layers. (B) Primitive neural tissues, including neural tube and neural rosettes. (C) Retinal epithelium. (D) Bundles of striated skeletal muscle-like tissue. (E) Gromerular-like structures. (F) Respiratory or gastrointestinal-like epithelium. (G) Glandular-like tissue. (F, G) Glycogen-depositing cells stained with Periodic Acid of Schiff. Nontransduced hIDPSCs did not form teratomas (data not shown). Magnifications: 4× (A); 20× (B–G). Scale bars: 400 μm (A); 50 μm (B–G).
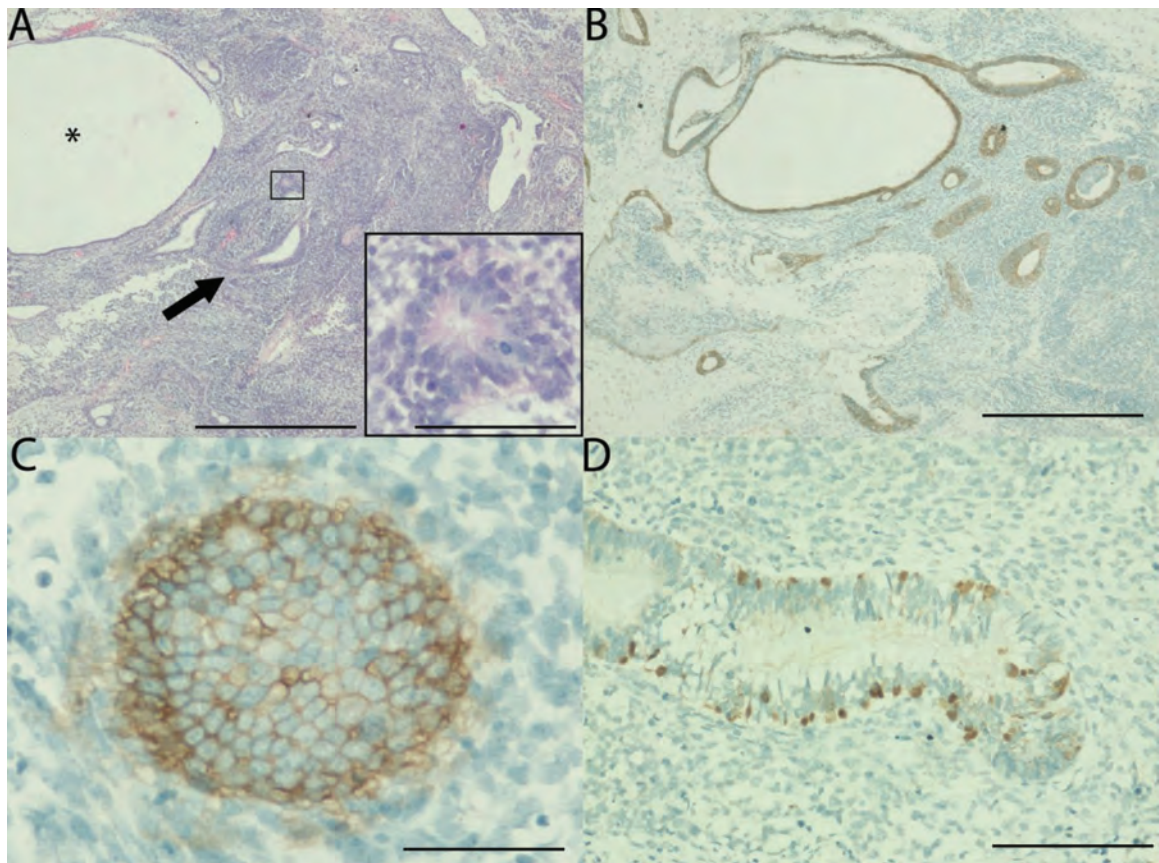
Figure 7. Histological and histochemical analyses of teratoma tissues from hIDPSC-iPSC7 5 weeks after intratesticle transplantation into nude mice. (A) Neural tissue derived from H&E-stained teratoma (inset higher magnification shows neural rosette). (B) Multiple sites of primitive neural tissues, including neural tube with positive staining for synaptophysin. (C) Enolase-positive neurosphere-like structures. (D) Synaptophysin-positive developing neural tube. Magnifications: 10× (A, B); 60× (C); 20× (D); 40× (inset in A). Scale bars: 250 μm (A, B); 20 μm (C); 80 μm (D); 10 μm (inset in A).

cially in the context of neurological disorders, when neural lineages from hIPSCs are needed for research involving effective treatment of these diseases (34).

While this manuscript was in preparation, an independent report (36) described the generation of iPSCs using heterogeneous populations of both DPSCs and SHED, which confirmed our findings that reprogramming efficiency depends on differentiation state of the cells. DPSCs and SHED are typical MSCs (9,24), but despite claims that they can be quickly reprogrammed to a pluripotent state, it required several attempts and two rounds of transfection to reprogram cells to improve efficiency (36). Moreover, DPSCs or SHED required a longer time period for initial colony formation (2–3 weeks more than other somatic cells) and teratoma formation when compared to hIDPSCs-iPSCs. Together with Yan et al. (36), our data confirm our previous observation that hIDPSCs are likely multipotent precursors of both DPSCs and SHED (14).

hIDPSC can be easily derived from dental pulp ex-

tracted from adult or "baby teeth" obtained during routine dental visits (14). Moreover, hIDPSC are immunologically privileged (an advantage for future HLA donor selection) and can be used in the absence of any immune suppression protocol (6,8,13). hIDPSC have potentially valuable cell therapy applications, including reconstruction of large cranial defects, production of chimeric myofibers in golden retriever muscular dystrophy dogs, and reconstruction of corneal epithelium in rabbits without presenting any graft rejection (6,8,13). The fact that hIDPSCs replicate fast indicates that they may carry less somatic mutations than terminally differentiated cells, such as fibroblasts. The fact that hIDPSCs can be easily isolated from tissue from the tooth of young patients offers another advantage compared to more invasive procedures, such as skin punch biopsies. Finally, to our knowledge, this is the first report of hiPSC complete derivation and characterization in Latin America, attesting to the feasibility of iPSC technology across laboratories around the world.

REFERENCES

1. Aasen, T.; Raya, A.; Barrero, M. J.; Garreta, E.; Consiglio, A.; Gonzalez, F.; Vassena, R.; Bilic, J.; Pekarik, V.; Tiscornia, G.; Edel, M.; Boue, S.; Belmonte, J. C. I. Efficient and rapid generation of induced pluripotent stem cells from human keratinocytes. Nat. Biotechnol. 26(11): 1276–1284; 2008.

2. Aoi, T.; Yae, K.; Nakagawa, M.; Ichisaka, T.; Okita, K.; Takahashi, K.; Chiba, T.; Yamanaka, S. Generation of pluripotent stem cells from adult mouse liver and stomach cells. Science 321(5889):699–702; 2008.

3. Calhoun, M. E.; Jucker, M.; Martin, L. J.; Thinakaran, G.; Price, D. L.; Mouton, P. R. Comparative evaluation of synaptophysin-based methods for quantification of synapses. J. Neurocytol. 25(12):821–828; 1996.

4. Carvajal-Vergara, X.; Sevilla, A.; D'Souza, S. L.; Ang, Y. S.; Schaniel, C.; Lee, D. F.; Yang, L.; Kaplan, A. D.; Adler, E. D.; Rozov, R.; Ge, Y.; Cohen, N.; Edelmann, L. J.; Chang, B.; Waghray, A.; Su, J.; Pardo, S.; Lichtenbelt, K. D.; Tartaglia, M.; Gelb, B. D.; Lemischka, I. R. Patient-specific induced pluripotent stem-cell-derived models of LEOPARD syndrome. Nature 465(7299):808–812; 2010.

5. Cooke, M. J.; Stojkovic, M.; Przyborski, S. A. Growth of teratomas derived from human pluripotent stem cells is influenced by the graft site. Stem Cells Dev. 15(2):254–259; 2006.

6. de Mendonça Costa, A.; Bueno, D. F.; Martins, M. T.; Kerkis, I.; Kerkis, A.; Fanganiello, R. D.; Cerruti, H.; Alonso, N.; Passos-Bueno, M. R. Reconstruction of large cranial defects in nonimmunosuppressed experimental design with human dental pulp stem cells. J. Craniofac. Surg. 19(1):204–210; 2008.

7. Eminli, S.; Utikal, J.; Arnold, K.; Jaenisch, R.; Hochedlinger, K. Reprogramming of neural progenitor cells into induced pluripotent stem cells in the absence of exogenous Sox2 expression. Stem Cells 26(10):2467–2474; 2008.

8. Gomes, J.; Monteiro, B. G.; Melo, G. B.; Smith, R. L.; Silva, M. C.; Lizier, N. F.; Kerkis, A.; Cerruti, H.; Kerkis, I. Corneal reconstruction with tissue-engineered cell sheets composed of human immature dental pulp stem cells. Invest. Ophthalmol. Vis. Sci. 51(3):1408–1414; 2009.

9. Gronthos, S.; Mankani, M.; Brahim, J.; Robey, P. G.; Shi, S. Postnatal human dental pulp stem cells (DPSCs) in vitro and in vivo. Proc. Natl. Acad. Sci. USA 97(25): 13625–13630; 2000.

10. Hanna, J.; Markoulaki, S.; Schorderet, P.; Carey, B. W.; Beard, C.; Wernig, M.; Creyghton, M. P.; Steine, E. J.; Cassady, J. P.; Foreman, R.; Lengner, C. J.; Dausman, J. A.; Jaenisch, R. Direct reprogramming of terminally differentiated mature B lymphocytes to pluripotency. Cell 133(2):250–264; 2008.

11. Huang, A. H.; Chen, Y. K.; Lin, L. M.; Shieh, T. Y.; Chan, A. W. Isolation and characterization of dental pulp stem cells from a supernumerary tooth. J. Oral Pathol. Med. 37(9):571–574; 2008.

12. Huangfu, D.; Osafune, K.; Maehr, R.; Guo, W.; Eijkelenboom, A.; Chen, S.; Muhlestein, W.; Melton, D. A. Induction of pluripotent stem cells from primary human fibroblasts with only Oct4 and Sox2. Nat. Biotechnol. 26(11): 1269–1275; 2008.

13. Kerkis, I.; Ambrosio, C. E.; Kerkis, A.; Martins, D. S.; Zucconi, E.; Fonseca, S. A.; Cabral, R. M.; Maranduba, C. M.; Gaiad, T. P.; Morini, A. C.; Vieira, N. M.; Brolio, M. P.; Sant'Anna, O. A.; Miglino, M. A.; Zatz, M. Early transplantation of human immature dental pulp stem cells from baby teeth to golden retriever muscular dystrophy (GRMD) dogs: Local or systemic? J. Transl. Med. 6(35): 1–13; 2008.

14. Kerkis, I.; Kerkis, A.; Dozortsev, D.; Stukart-Parsons, C. P.; Massironi, S. M. G.; Pereira, L. V.; Caplan, A. I.; Cerruti, H. F. Isolation and characterization of a population of immature dental pulp stem cells expressing OCT-4 and other embryonic stem cells markers. Cells Tissues Organs 184(3–4):105–116; 2006.

15. Kim, J. B.; Sebastiano, V.; Wu, G.; Araúzo-Bravo, M. J.; Sasse, P.; Gentile, L.; Ko, K.; Ruau, D.; Ehrich, M.; van den Boom, D.; Meyer, J.; Hübner, K.; Bernemann, C.; Ortmeier, C.; Zenke, M.; Fleischmann, B. K.; Zaehres, H.; Schöler, H. R. Oct4-induced pluripotency in adult neural stem cells. Cell 136(3):411–419; 2009.

16. Kim, J. B.; Zaehres, H.; Wu, G.; Gentile, L.; Ko, K.; Sebastiano, V.; Araüzo-Bravo, M. J.; Ruau, D.; Han, D. W.; Zenke, M.; Schöler, H. R. Pluripotent stem cells induced from adult neural stem cells by reprogramming with two factors. Nature 454(7204):646–650; 2008.

17. Kishi, Y.; Tanaka, Y.; Shibata, H.; Nakamura, S.; Takeuchi, K.; Masuda, S.; Ikeda, T.; Muramatsu, S.; Hanazono, Y. Variation in the incidence of teratomas after the transplantation of nonhuman primate ES cells into immunodeficient mice. Cell Transplant. 17(9):1095–1102; 2008.

18. Li, H.; Collado, M.; Villasante, A.; Strati, K.; Ortega, S.; Ca?amero, M.; Blasco, M. A.; Serrano, M. The Ink4/Arf locus is a barrier for iPS cell reprogramming. Nature 460(7259):1085–1086; 2009.

19. Loh, Y. H.; Agarwal, S.; Park, I. H.; Urbach, A.; Huo, H.; Heffner, G. C.; Kim, K.; Miller, J. D.; Ng, K.; Daley, G. Q. Generation of induced pluripotent stem cells from human blood. Blood 113(22):5476–5479; 2009.

20. Maherali, N.; Hochedlinger, K. Guidelines and techniques for the generation of induced pluripotent stem cells. Cell Stem Cell 3(6):595–605; 2008.

21. Marchetto, M. C.; Carromeu, C.; Acab, A.; Yu, D.; Yeo, G. W.; Mu, Y.; Chen, G.; Gage, F. H.; Muotri, A. R. A model for neural development and treatment of rett syndrome using human induced pluripotent stem cells. Cell 143(4):527–539; 2010.

22. Marchetto, M. C.; Yeo, G. W.; Kainohana, O.; Marsala, M.; Gage, F. H.; Muotri, A. R. Transcriptional signature and memory retention of human-induced pluripotent stem cells. PLoS One 4(9):e7076; 2009.

23. Martin, M. J.; Muotri, A.; Gage, F.; Varki, A. Human embryonic stem cells express an immunogenic nonhuman sialic acid. Nat. Med. 11(2):228–232; 2005.

24. Miura, M.; Gronthos, S.; Zhao, M.; Lu, B.; Fisher, L. W.; Robey, P. G.; Shi, S. SHED: Stem cells from human exfo-

liated deciduous teeth. Proc. Natl. Acad. Sci. USA 100(10):5807–5812; 2003.

25. Muotri, A. R.; Marchetto, M. C.; Suzuki, M. F.; Okazaki, K.; Lotfi, C. F.; Brumatti, G.; Amarante-Mendes, G. P.; Menck, C. F. Low amounts of the DNA repair XPA protein are sufficient to recover UV-resistance. Carcinogenesis 23(6):1039–1046; 2002.

26. Nam, H.; Lee, G. Identification of novel epithelial stem cell-like cells in human deciduous dental pulp. Biochem. Biophys. Res. Commun. 386(1):135–139; 2009.

27. Navarro-Alvarez, N.; Soto-Gutierrez, A.; Yuasa, T.; Yamatsuji, T.; Shirakawa, Y.; Nagasaka, T.; Sun, S. D.; Javed, M. S.; Tanaka, N.; Kobayashi, N. Long-term culture of Japanese human embryonic stem cells in feeder-free conditions. Cell Transplant. 17(1–2):111–119; 2008.

28. Park, I. H.; Zhao, R.; West, J. A.; Yabuuchi, A.; Huo, H.; Ince, T. A.; Lerou, P. H.; Lensch, M. W.; Daley, G. Q. Reprogramming of human somatic cells to pluripotency with defined factors. Nature 451(7175):141–146; 2008.

29. Siqueira da Fonseca, S. A.; Abdelmassih, S.; Lavagnolli, T. M. C.; Serafim, R. C.; Clemente Santos, E. J.; Mota Mendes, C.; de Souza Pereira, V.; Ambrosio, C. E.; Miglino, M. A.; Visintin, J. A.; Abdelmassih, R.; Kerkis, A.; Kerkis, I. Human immature dental pulp stem cells contribution to developing mouse embryos: Production of human/mouse preterm chimaeras. Cell Prolif. 42(2):132–140; 2009.

30. Sun, N.; Panetta, N. J.; Gupta, D. M.; Wilson, K. D.; Lee, A.; Jia, F.; Hu, S.; Cherry, A. M.; Robbins, R. C.; Longaker, M. T.; Wu, J. C. Feeder-free derivation of induced pluripotent stem cells from adult human adipose stem cells. Proc. Natl. Acad. Sci. USA 106(37):15720–15725; 2009.

31. Takahashi, K.; Tanabe, K.; Ohnuki, M.; Narita, M.; Ichisaka, T.; Tomoda, K.; Yamanaka, S. Induction of pluripotent stem cells from adult human fibroblasts by defined factors. Cell 131(5):861–872; 2007.

32. Takahashi, K.; Yamanaka, S. Induction of pluripotent stem cells from mouse embryonic and adult fibroblast cultures by defined factors. Cell 126(4):663–676; 2006.

33. Takenaka, C.; Nishishita, N.; Takada, N.; Jakt, L. M.; Kawamata, S. Effective generation of iPS cells from CD34+ cord blood cells by inhibition of p53. Exp. Hematol. 38:154–162; 2010.

34. Torrente, Y.; Polli, E. Mesenchymal stem cell transplantation for neurodegenerative diseases. Cell Transplant. 17(10–11):1103–1113; 2008.

35. Yamanaka, S. A fresh look at iPS cells. Cell 137(1):13–17; 2009.

36. Yan, X.; Qin, H.; Qu, C.; Tuan, R. S.; Shi, S.; Huang, G. T. J. iPS cells reprogrammed from mesenchymal-like stem/progenitor cells of dental tissue origin. Stem Cells Dev. 19(4):469–480; 2010.

37. Ye, Z.; Zhan, H.; Mali, P.; Dowey, S.; Williams, D. M.; Jang, Y.; Dang, C. V.; Spivak, J. L.; Moliterno, A. R.; Cheng, L. Human-induced pluripotent stem cells from blood cells of healthy donors and patients with acquired blood disorders. Blood 114(27):5473–5480; 2009.